Widespread gravity changes accompanying rapid uplift at Laguna del Maule, Chile

Craig Miller[a], Glyn Williams-Jones[a], Hélène Le Mével[b], Basil Tikoff[b]

a. Simon Fraser University *b.* University of Wisconsin-Madison

cam32@sfu.ca

Introduction

Laguna Del Maule Volcanic Field

- Will this be the world's next caldera forming eruption?
- Active since 1.5 Ma producing at least 130 distinct vents.
- 36 eruptions post glaciation from 24 vents, high silica rhyolite (*Hildreth et al.*, 2010).
- Most recent rhyolite dated at 2.2 ka.
- Currently the world's fastest inflating volcano that is not actually in eruption.
- Deformation first detected in 2007 from InSAR at rates of up to 250 mm/year.
- Our hypothesis is that uplift is due to intrusion of basaltic magma into the base of a rhyolitic magma chamber.
- In 2013 we began a microgravity and deformation study to test this hypothesis.

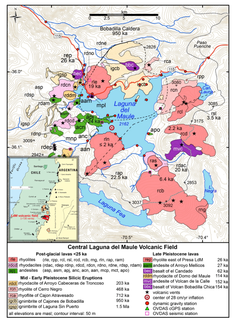

Figure 1: Geological map of Laguna del Maule, Chile, with location inset.

Survey Method

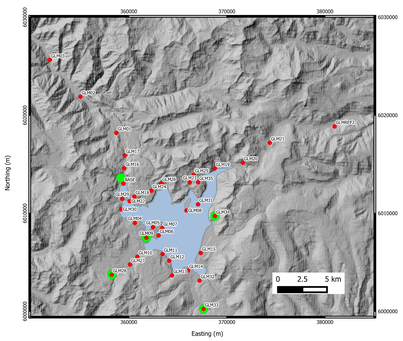

Figure 2: Digital Elevation Model of Laguna Del Maule. Red dots are microgravity stations. Green circles are CGPS stations.

- A 35 benchmark mirogravity network established in March 2013 and resurveyed in January 2014 (Figure 2).
- Benchmarks precisely positioned with static GNSS, corrected with network of 5 CGPS stations around LdM.
- 3 gravity meters employed to minimise errors from an individual meter.
- Data corrected for Earth tides, ocean loading and up to 294 mm of uplift (Δh) between the two surveys. Data corrected to account for change in lake level between the two surveys (lake level correction, llc). Maximum llc = 11 μGal.
- Residual gravity anomaly Δg_{res} = Δg_{obs} - (FAG x Δh) - llc.
- We assume spherical source and ignore the deformation effect.
- Δg_{res} standard error varies from 19 μGal to 108 μGal, averaging 28 μGal.

Height Change

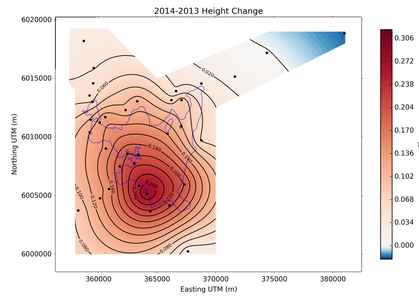

Figure 4: Height change (Δh) between 2013 and 2014 surveys. Black dots are survey stations, blue line is lake outline, contour interval 0.02 m.

- Benchmark height changes between 2013 and 2014 show a **maximum uplift of 281±13 mm**, centered in the south of the lake (Figure 4).
- Height errors range from 2 mm to 25 mm to a maximum 79 mm.
- Uplift pattern is roughly circular around the maximum with a slight NW-SE elongation.

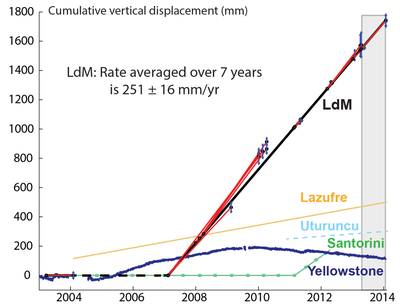

Figure 5: Deformation timeseries from LdM from 2003 to 2014, derived from InSAR (*Feigl et al.*, 2014). Microgravity survey period in grey shading. Figure modified from *Singer* (2014).

- Figure 5 shows deformation time series since 2004 in comparison to other inflating volcanic systems.

Gravity Change

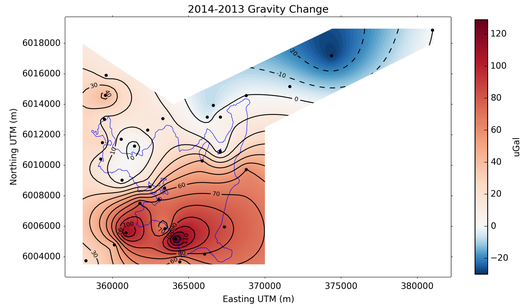

Figure 3: Residual gravity (Δg_{res}) between 2013 and 2014 surveys. Black dots are survey stations, blue line is lake outline, contour interval 10 μGal.

- Residual gravity change between surveys has a **maximum Δg of 134 ± 30 μGal** (Figure 3).
- Two sample, bootstrap t-test, on all the data, shows 2013 and 2014 gravity surveys are different at p <0.01
- The Δg anomaly is oriented east-west and covers an area of 5 km x 10 km in the southern half of the lake.
- **1.2 x 10^{11} kg estimated minimum mass increase** from Gaussian integration of the residual gravity anomaly.
- **Source depth range of 2-4 km** from half amplitude / half width relationships for spherical source.
- Localised, small positive and negative anomalies may relate to mass changes caused by roadworks near the benchmarks.

Future Work

- Resurvey the network in 2015 and 2016 to assess the continuation of temporal changes.
- Quantitatively model the gravity changes to determine the shape, density and depth of the intrusion.
- Jointly invert the gravity and height data to determine the spatial relationships between the volumetric and mass sources. How to reconcile the differences in source depths?
- Undertake Bouguer gravity survey to model internal structure.
- Undertake CO_2 soil gas survey to help constrain magma input into system.

Gravity and Height relationships

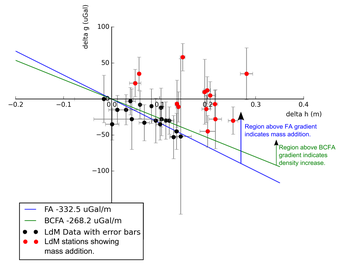

Figure 6: Δg_{obs} + llc vs Δh with error bars (standard error of mean). Red dots are those stations which show mass increase outside of the error in measurement.

- FA = Δg_{obs} + llc / Δh ; BCFA = FA + 4/3*Pi*Gx10^8*ρ (*Williams-Jones and Rymer*, 2002)
- Figure 6 shows 14 stations locate beyond error, above the free air gradient (FA), indicating mass addition. These stations also lie above the Bouguer corrected FA, (BCFA), for a spherical source of density 2300 kg/m^3 indicating that the system has also increased in density at these locations.

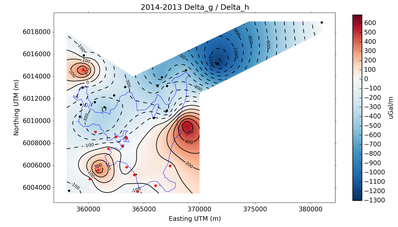

Figure 7: Δg_{obs} + llc / Δh spatial relationship. Red dots are the same as in Figure 6, indicating mass addition and density increase at these stations.

- Figure 7 shows spatial distribution of gravity and height change ratios indicating mass increase in southern part of the lake.

Discussion

- *Feigl et al.* (2014) modelled the inflation using InSAR during the period preceding the start of the gravity campaign. For the period 2010 to 2012 they calculated a volume change of **51±5 x 10^6 m^3/year** for a sill located **at 4.9 km depth**.
- Given height changes rates are constant from 2010 to 2014 we compare the InSAR sill volumetric source to a mass source derived from the gravity data.
- We calculate the equivalent volume change from the gravity data, assuming a density of 2700 kg/m^3 for a basaltic magma intrusion. We ignore for the moment possible effects of magma compressibility (*Rivalta and Segall*, 2008).

$$\Delta V_{Gravity} = \Delta m/\rho = 1.2x\ 10^{11}\ /\ 2700 = \mathbf{44\ x\ 10^6\ m^3}$$

- InSAR volumetric source volume and gravity mass volume agree.
- MT data (M. Unsworth *pers comm*) shows a conductor at ~3 km, similar to the depth of the gravity source.
- To test whether the location and thickness of the volumetric source can reproduce the observed gravity anomaly, we filled the InSAR sill volume with material of density 2700 kg/m^3 and calculated the gravity effect. This model produced a gravity change of only ~3 μGal which is below the survey detection limit.
- The gravity anomaly is more compact than the deformation anomaly with most of the mass localised in the southern half of the lake (and in the southern half of the volumetric source).

Conclusions

- Widespread mass and density increase beneath southern part of Laguna del Maule accompanies uplift.
- Volumetric source and mass volumes broadly agree but sources may be spatially distinct.
- If rate of volume change has been constant then up to 0.3 km^3 of magma has been intruded since 2007.
- Gravity anomaly coincident with most recent rhyolite flow: possible long lived area of melt.

Acknowledgements

- Field work was funded by NSF RAPID grant EAR-1322595.
- Thanks to Nathan Andersen (UW) for field assistance, and the dates in Introduction.
- H.L.M. has been partially supported by NASA grant (NASA-NNX12AO37G) , the G.P. Woollard fund, and NSF-1411779.
- C.A.M. is supported by GNS Science, EQC and Mitacs, with acknowledgments to Mira Geoscience.

References

Feigl, K. L., H. Le Mevel, S. Tabrez Ali, L. Cordova, N. L. Andersen, C. DeMets, and B. S. Singer, Rapid uplift in Laguna del Maule volcanic field of the Andean Southern Volcanic zone (Chile) 2007-2012, *Geophysical Journal International*, *196*(2), 885–901, doi:10.1093/gji/ggt438, 2014.

Hildreth, W., E. Godoy, J. Fierstein, and B. Singer, Laguna Del Maule Volcanic Field: Eruptive history of a Quaternary basalt-to-rhyolite distributed volcanic field on the Andean rangecrest in central Chile, *Servicio Nacional de Geologia y Mineria, Boletin*, *63*, 145, 2010.

Rivalta, E., and P. Segall, Magma compressibility and the missing source for some dike intrusions, *Geophysical Research Letters*, *35*(4), L04,306, doi:10.1029/2007GL032521, 2008.

Singer, B. S., Laguna del Maule, *GSA Today*, 2014.

Williams-Jones, G., and H. Rymer, Detecting volcanic eruption precursors: a new method using gravity and deformation measurements, *Journal of Volcanology and Geothermal Research*, *113*, 379–389, 2002.